CARDIFF UNIVERSITY

PRIFYSGOL CAERDYDD

12th Association of Computational Mechanics in Engineering

Annual Conference

Cardiff School of Engineering, 5th – 6th April 2004

ACME 2004

ACME 2004 Local Organising Team, Cardiff

Professor Hywel R. Thomas (Head of School of Engineering)
Dr. Stephen Rees (Vice Chair)
Dr. Terry Bennett
Dr. Anthony Jefferson
Ms Cherrie Summers
Ms Aderyn Reid

ACME Committee:

Emeritus Professor Oleg C Zienkiewicz	(Honorary President)
Dr. Marcus A. Wheel	(Chairman)
Dr. S. W. Rees	(Vice Chairman)
Dr Edward A W Maunder	(Honorary Treasurer)
Dr Andrew Chan	(Honorary Secretary)

Dr. Chris Bailey
Professor Peter Bettess
Professor Nenad Bicanic
Prof. Javier Bonet
Professor Mark Cross
Dr. Alojz Ivankovic
Professor Roland W Lewis
Professor D Roger J Owen
Professor Ian Smith

Tuesday 6th April 2004

9:00 am – 10:40am Session 5a, Main Lecture Theatre (South 1.32)

9:00 – 9:20 A Thermodynamic Approach to Constitutive Modelling of Concrete
G.D. Nguyen and G.T. Houlsby.

9:20 – 9:40 Two-component contact for embedded planes in a 3D plastic-damage-contact constitutive model.
S. C. Hee and A.D. *Jefferson*

9:40 – 10:00 Size and Parabolic-Shape Optimization of Dome Structures with Buckling and Load Variation on the Joints Using Genetic Algorithm
M.R. Ghasemi and F. Azhdari

10:00 – 10:20 Constitutive Behaviour of a Pressure and Lode-Sensitive Material: Multiaxial Stiffness Change and Instabilities.
Roger Crouch and Mihail Petkovski

10:20 – 10:40 Recent developments in computational fracture mechanics at Cardiff
Q.Z. Xiao and B.L. Karihaloo.

10:40 – 11:10 Coffee Break, Room South 4.10(A)

9:00am – 10:40pm Session 5b, Lecture Theatre T4 (South 1.25)

9:00 – 9:20 Design Sensitivity of a Sequentially Coupled Problem: Casting.
R. Ahmad, D.T. Gethin, R.W. Lewis and E.W. Postek

9:20 – 9:40 Formulation of Lower Bound Limit Analysis as a Second Order Cone Programming (SOCP) Problem
A. Makrodimopoulos and C.M. Martin.

9:40 – 10:00 Finite element model of mould filling during squeeze forming processes.
E.W. Postek, R.W. Lewis, D.T. Gethin, R.S. Ransing.

10:00 – 10:20 Turbulence Modelling for Thermal Management of Electronic Systems
K. Dhinsa, C. Bailey, and K. Pericleous

10:20 – 10:40 Simulation of deformation of ductile pharmaceutical particles with finite element method.
L.L. Dong, R.W. Lewis, D.T. Gethin, and E.W. Postek.

10:40 – 11:10 Coffee Break, Room South 4.10(A)

Simulation of deformation of ductile pharmaceutical particles with finite element method

L.L. Dong*, R.W. Lewis, D.T. Gethin, E.W. Postek
Department of Mechanical Engineering
University of Wales Swansea
Swansea SA2 8PP
* corresponding author (L.L. Dong)

1. INTRODUCTION

In order to guarantee the strength and thus the quality of the tablets produced during the tabletting process, it is essential to understand the deforming characteristics of excipient binders. The present numerical work is motivated to provide an insight into the mechanical behaviour of the particle deformation of the excipient binder. In the present study pregelatinised starch is selected, which is known to behave in a ductile manner during compaction.

An elasto-viscoplastic material model has been selected in the present study to simulate the deformation behaviour of the pregelatinised starch. Elasto-viscoplastic model is chosen because all the plastic deformation exhibits rate-dependency to some extent, and it is a well-developed model for simulating non-linear deformation which has been studied for four decades (Perzyna (1966), Zabaras and Arif (1992)).

2. NUMERICAL MODEL AND PROCEDURE

2.1. Governing Equations and Finite Element Formulation

In the present study, the deformation of the starch particles during the tabletting process is described by the dynamic equilibrium equation. By using the Principle of Virtual Work, the following weak form of the dynamic equilibrium equation, at time t_n, can be obtained:

$$\int_\Omega [\delta\boldsymbol{\varepsilon}_n]^T \boldsymbol{\sigma}_n d\Omega - \int_\Omega [\delta\mathbf{u}_n]^T [\mathbf{b}_n - \rho_n \ddot{\mathbf{u}}_n - c_n \dot{\mathbf{u}}_n] d\Omega - \int_{\Gamma_t} [\delta\mathbf{u}_n]^T \mathbf{T}_n d\Gamma = 0 \qquad (1)$$

where the subscript n indicates the quantities of all the relevant variables at time instant t_n (This is also valid in all of the following equations, where this subscript is omitted for brevity), $\boldsymbol{\sigma}$ is the vector of stresses, $\mathbf{u}$ is the vector of displacement, $\delta\mathbf{u}$ is the vector of virtual displacements, $\delta\boldsymbol{\varepsilon}$ is the vector of associated virtual strains, $\mathbf{b}$ is the vector of applied body forces, $\mathbf{T}$ is the vector of surface tractions, $\dot{\mathbf{u}}$ is the vector of velocities, $\ddot{\mathbf{u}}$ is the vector of accelerations, ρ is the mass density, c is the damping coefficient, Ω is the calculation domain, Γ is the boundary of the domain, and Γ_t is the part of the boundary on which boundary tractions are prescribed.

By introducing the shape functions, the governing equation (1) can be rewritten in matrix form as follows:

$$\mathbf{M}\ddot{\mathbf{d}}_n + \mathbf{C}\dot{\mathbf{d}}_n + \mathbf{p}_n = \mathbf{f}_n \qquad (2)$$

where $\mathbf{M}$ and $\mathbf{C}$ are the global mass and damping matrices respectively, $\ddot{\mathbf{d}}$ is the global vector of nodal accelerations, $\dot{\mathbf{d}}$ is the global vector of nodal velocities, $\mathbf{p}$ is the global vector of internal resisting nodal forces and $\mathbf{f}$ is the vector containing the applied consistent nodal forces and surfaces traction forces.

2.2. Elasto-Viscoplastic Theory

Two basic assumptions are made in elasto-viscoplasticity theory (Prager (1961)). i.e.,

$$\dot{\boldsymbol{\varepsilon}}_n = [\dot{\boldsymbol{\varepsilon}}_e]_n + [\dot{\boldsymbol{\varepsilon}}_{vp}]_n$$

(3)

The onset of viscoplastic behaviour is governed by the scalar yield condition,

$$F(\boldsymbol{\sigma}_n, [\boldsymbol{\varepsilon}_{vp}]_n) - Y = 0$$

(4)

where Y is the uniaxial yield stress which may itself be a function of a hardening parameter. It is assumed that viscoplastic flow occurs when $F(\boldsymbol{\sigma}_n, [\boldsymbol{\varepsilon}_{vp}]_n) > Y$.

By assuming that the plastic flow is associative plasticity, we have

$$[\dot{\boldsymbol{\varepsilon}}_{vp}]_n = \gamma \langle \Phi(F) \rangle \frac{\partial F}{\partial \boldsymbol{\sigma}_n}$$

(5)

The following complete constitutive relationship can be obtained:

$$\dot{\boldsymbol{\varepsilon}}_n = [\mathbf{D}]^{-1} [\dot{\boldsymbol{\sigma}}]_n + \gamma \langle \Phi_n(F) \rangle \frac{\partial F}{\partial \boldsymbol{\sigma}_n} \tag{6}$$

The Von Mises yield criterion is employed to determine the stress level at which plastic deformation starts.

2.3. Adaptive Remeshing Algorithm

The Zienkiewicz-Zhu error estimator is used and the adaptive remeshing is performed when the following global error η is larger than a prescribed permissible value η_{perm}, i.e.,

$$\eta = \frac{\left[\int_\Omega (\boldsymbol{\sigma} - \hat{\boldsymbol{\sigma}})^T (\boldsymbol{\sigma} - \hat{\boldsymbol{\sigma}}) d\Omega\right]^{1/2}}{\left[\int_\Omega \boldsymbol{\sigma}^T \boldsymbol{\sigma}\, d\Omega\right]^{1/2}}$$

(7)

where $\boldsymbol{\sigma}$ and $\mathbf{u}$ represent the exact values of the stresses and displacements, while $\hat{\boldsymbol{\sigma}}$ and $\hat{\mathbf{u}}$ are the finite element approximations, respectively.

The mesh refinement is carried out when $\eta > \eta_{perm}$.

3. APPLICATIONS AND RESULTS

3.1. Problem Description

The ductile excipient material selected in the present study is pregelatinised starch. The major material properties are summarized in Table 1.

Table 1. Summary of the pregelatinised Starch Properties

Young's Modulus, E (N/m^2)	5.315×10^{10}
Poission's Ratio, ν	0.3
The yielding stress, σ_{eff}^0 (N/m^2)	4.48×10^{8}
Density, ρ (Kg/m^3)	660.0
Particle diameter, d (m)	2.0×10^{-5}

3.2. Numerical Results and Discussions

3.2.1 Deformation with prescribed edge loading

The geometry of this case is shown in Fig. 1. The adaptive analysis begins with a coarse mesh of 254 elements producing a discretization error of 2.52. After three iteration of mesh refinement, the final mesh is reached with the discretization error reduced to 0.026. The final mesh contains 1593 elements. The final deformation based on the final mesh is shown in Fig. 2. It is observed that the refinement is mainly performed around the loading edge, where the concentrated stresses occur. The solutions obtained from the final mesh are shown in Fig. 4. The plastic deformation occurs in the area around the loading edge with the effective stress no less than σ_{eff}^{0}.

3.2.2 Deformation with prescribed displacement

The second case was selected to investigate the effectiveness of the present numerical algorithm for modelling deforming particles with prescribed displacements. In this case, the circular particle, which is supported on a rigid surface, with the bottom node fixed shown in the previous two cases is being pressed by a rigid flat plate from the top vertex of the particle. This configuration is shown in Fig. 5. After three adaptive iterations are performed, the global error of the final mesh was reduced to 2.2% containing 2483 elements. It could be observed from Fig. 6 that the refinement of the mesh is performed in the area around the squeezing plate, indicating higher gradients of stresses. It can be found from Fig. 8 that the maximum effective stresses occur at the locations close to the squeezing plate. In other sections of the particle away from the squeezing plate, the effective stress decreases gradually.

REFERENCES

Perzyna, P., Fundamental problems in viscoplasticity, Advances in Applied Mechanics (9), 243-377, 1966

Prager, W., Introduction to Mechanics of Continua, Ginn, Boston, USA, 1961

Zabaras, N., Arif, A.F.M., A family of integration algorithms for constitutive equations in finite deformation elasto-viscoplasticity, Int. J. for Numerical Methods in Engineering 33, 59-84, 1992

Zienkiewicz, O.C., and Cormeau, I.C., Visco-plasticity – plasticity and creep in elastic solids – a unified numerical solution approach, Int. J. Num. Meth. Engng. 8, 821-845, 1974

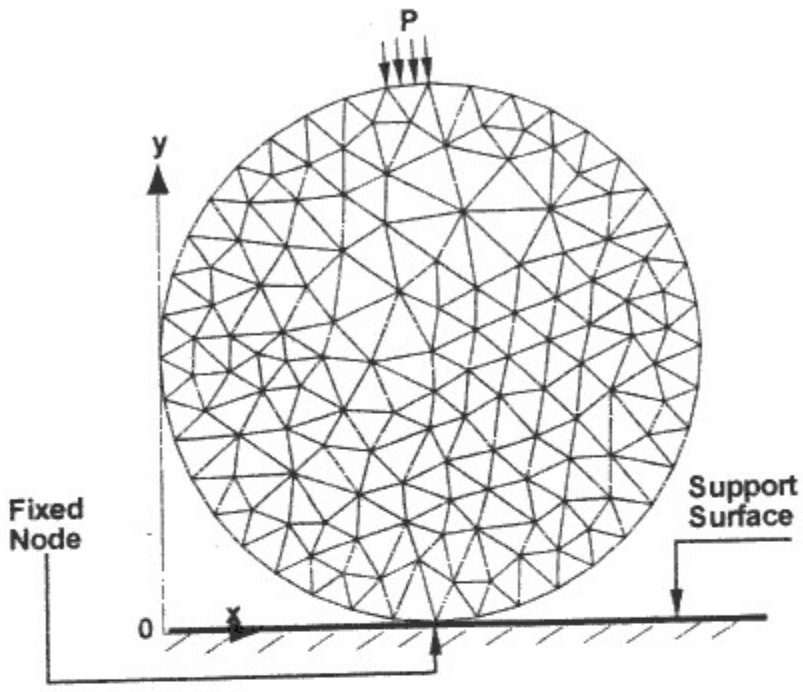

Fig. 1. Geometry of the particle subjected to loading on the edge

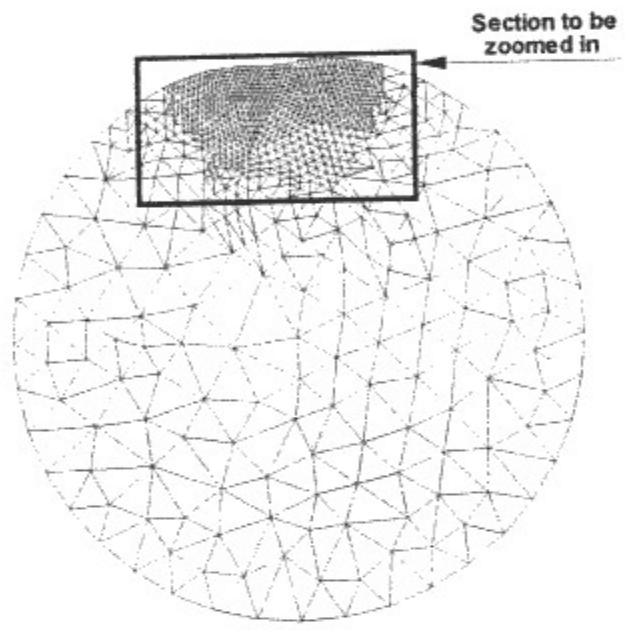

Fig. 2. Final mesh and final deformation (Number of elements = 1593; η = 2.6%)

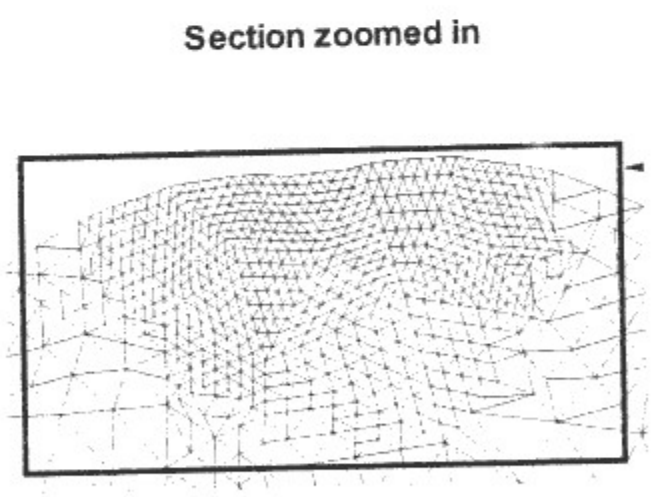

Fig. 3. Section being zoomed in

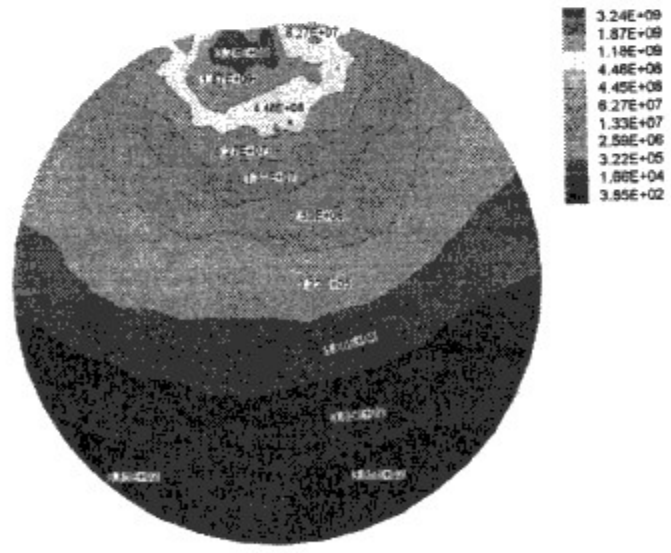

Fig. 4. Contour of the effective stress

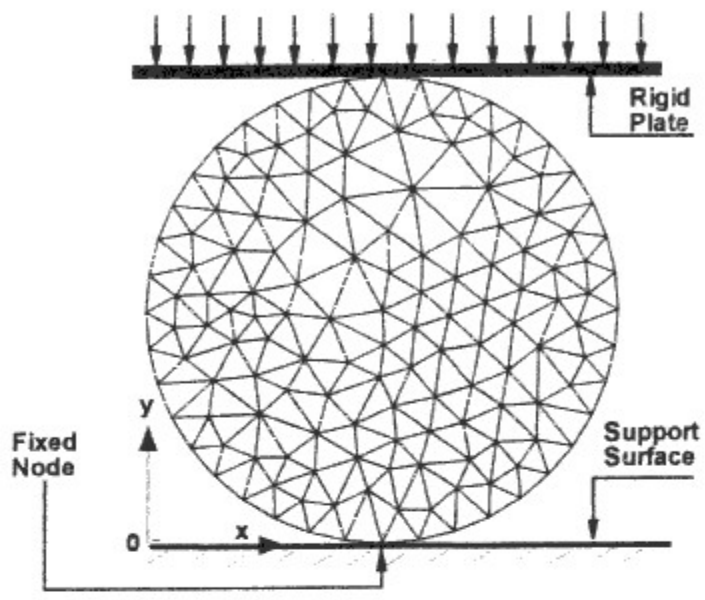

Fig. 5. Geometry of the particle subjected to plate squeezing

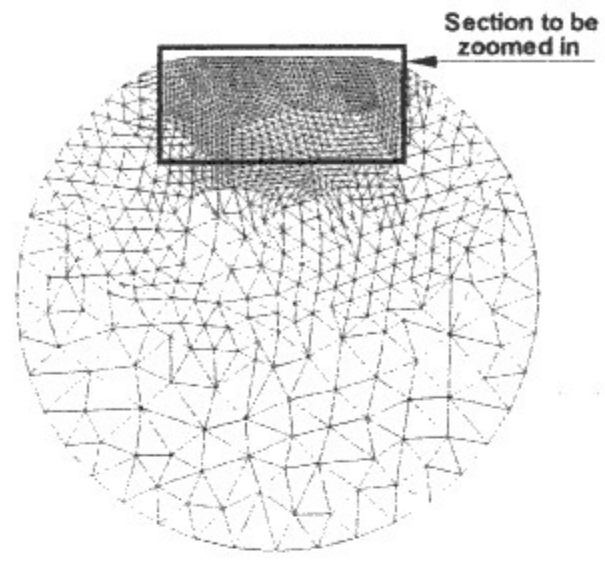

Fig. 6. Final mesh and final deformation (Number of elements = 2483; η = 2.2%)

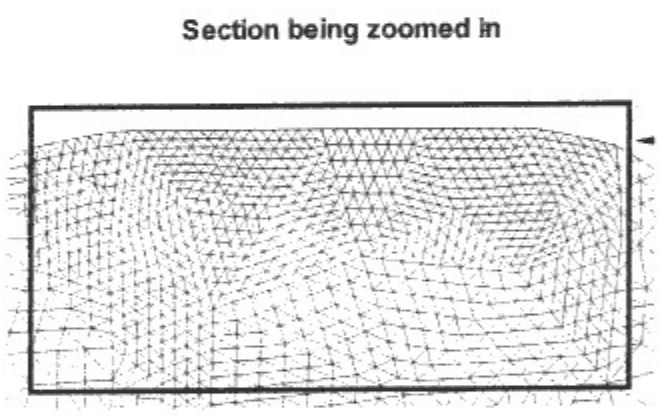

Fig. 7. Section being zoomed in

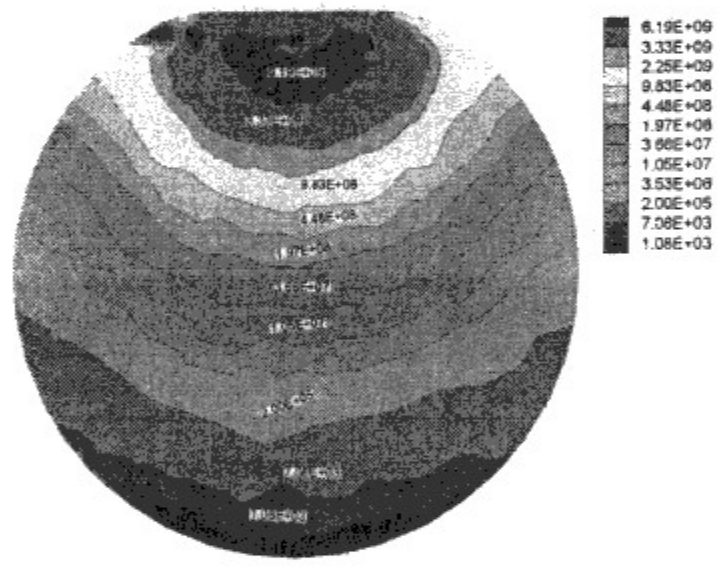

Fig. 8. Contour of the effective stress